IEEE Access
Multidisciplinary | Rapid Review | Open Access Journal

Received January 22, 2019, accepted February 16, 2019, date of publication March 7, 2019, date of current version April 3, 2019.

Digital Object Identifier 10.1109/ACCESS.2019.2903439

An Improved Sliding Mode Control Using Disturbance Torque Observer for Permanent Magnet Synchronous Motor

QI WANG[1,2], (Student Member, IEEE), HAITAO YU[1], (Member, IEEE), MIN WANG[3], AND XINBO QI[2]

[1]School of Electrical Engineering, Southeast University, Nanjing 210096, China
[2]Henan Institute of Technology, Xinxiang 453003, China
[3]School of Electrical Engineering, Zhengzhou University, Zhengzhou 450001, China

Corresponding author: Haitao Yu (htyu@seu.edu.cn)

This work was supported by the National Natural Science Foundation of China under Grant 41576096 and in part by the Foundation of Henan Educational Committee under Grant 17A120008.

ABSTRACT For the purpose of optimizing the speed control performance of the permanent magnet synchronous motor (PMSM) system, an adaptive sliding mode control (SMC) approach combining disturbance torque observer (DTO) is proposed during this paper. First, an improved sliding mode reaching law (SMRL) is introduced to reduce the sliding mode chattering. According to the choice of piecewise function term, the proposed SMRL adaptively selects the reaching velocity of the sliding mode. Then, the DTO is proposed to compensate for the effect of external disturbances. The DTO is used to produce a feed-forward signal, which is applied to the speed control loop, and the proposed SMRL is proved by Lyapunov law to ensure the stability of the whole system. Finally, the simulation and experiment results are implemented in Matlab2018a and TMS320F28335 (TI company's digital signal processor, DSP), respectively. The simulation and experimental results indicate the availability of the proposed SMC approach.

INDEX TERMS Sliding mode control (SMC), permanent magnet synchronous motor (PMSM), disturbance torque observer (DTO), sliding mode reaching law (SMRL).

I. INTRODUCTION

There are many excellent performance features of permanent magnet synchronous motors (PMSMs) such as high torque, power density and high efficiency, etc [1]. PMSMs are widely used in hybrid electric vehicles, wind power generators, industrial servo drives, etc. Due to the simplicity and ease of understanding, the conventional proportional-integral (PI) controller is still popular in actual PMSM system [2]. However, recent studies show that such control strategy has been experiencing some bottlenecks, such as the optimal PI coefficients are difficult to obtain, the contradiction between stability and performance, robustness to the variations of model parameters and external disturbances, etc., [3], proposed three reaching [4]. To overcome these obstacles, various nonlinear control methods have been proposed to improve the control performances, such as fuzzy logic control [5], sliding mode control [6], predictive control [7], neural network control [8], adaptive control [2], and so on. The SMC is a preferred research topic in the above mentioned nonlinear control methods, because its insensitivity to external disturbances and internal variations of parameter can guarantee perfect control performance. In [9], an adaptive dynamic sliding mode controller was proposed for the rotor position control of induction motor. Paper [10] has proposed a novel rotor position sliding mode observer for SPMSM drives. In [11], a fixed switching period sliding mode current controller was proposed for direct torque control (DTC) system of PMSM.

However, chattering phenomenon does exist in the SMC method, while the robustness of this control method can only be ensured by using large control gains. Thus, in order to reduce the chattering phenomena, numerous methods have been adopted, such as higher-order sliding mode control method [12]–[14], complementary sliding mode control method and reaching law method [15], [16], continuous approximation technique [17]. Because of nonideal reaching

The associate editor coordinating the review of this manuscript and approving it for publication was Alfeu J. Sguarezi Filho.

at the terminal of the sliding surface, the chattering phenomenon occurred. Reaching law approach can directly deal with the arrival process to reduce the sliding mode chattering.

The literature [18] proposed three reaching laws: constant rate reaching law, constant plus proportional rate reaching law, and power rate reaching law. Then, Gao *et al.* [19] extended reaching law approach to the discrete time domain, and the reaching law approach is highly appreciated by domestic and foreign scholars [20]–[23]. The literature [24] proposed a no switching type reaching law, which can improve robustness of the control system. Ma *et al.* [25] proposed a novel exponential reaching law for driving the piezoelectric actuator. The experiments validate that the proposed approach is effective. The literature [26] designed a maximum power point tracking control approach consists of an improved reaching law and an integral sliding mode surface for the permanent magnet synchronous generator (PMSG). This proposed controller can restrain output voltage's ripple effectively. Mozayan *et al.* [27] proposed a SMC method for permanent magnet synchronous generator of wind turbine according to the enhanced exponential reaching law. The proposed reaching law can reduce chattering of SMC and improve the total property of harmonic distortion.

Obey the aforementioned reaching laws, small sliding mode gain can reduce chattering phenomenon, but with long reaching time. Reaching time to sliding mode surface and chattering is the main contradiction of conventional reaching law approach. To solve the above problems, in this paper, an improved sliding mode reaching law (SMRL), based on the option of piecewise function term, is proposed. The proposed SMRL can not only suppress the chattering but also reduce reaching time by fitting the variations of system states and the sliding mode surface. At the same time, to enhance disturbance rejection performance of this proposed SMC approach, an extended disturbance torque observer (DTO) is used. In this frame, a composite control method combining proposed SMRL and a feed-forward signal produced by disturbance torque observer applied to the speed control loop, which used to improve the speed performance of PMSM, called SMC+DTO, is developed.

Compared with other control approaches, this paper has the following contributions:

1) An improved reaching law, which can not only suppress the chattering but also reduce reaching time by adapting to the variations of system states and the sliding mode surface, is selected. In order to force the system converge to the equilibrium state, improved SMC control law based on this reaching law is designed.
2) The proposed SMC method which using an improved SMRL to ensure the stability of the whole system, is proved by Lyapunov theorem. Moreover, an extended disturbance torque observer, which can produce a feed-forward signal to optimize the speed control performance of PMSM, is used.
3) The proposed approach was simulated in Matlab2018a and implemented in TMS320F28335 platform. The results indicate the availability of the proposed SMC approach.

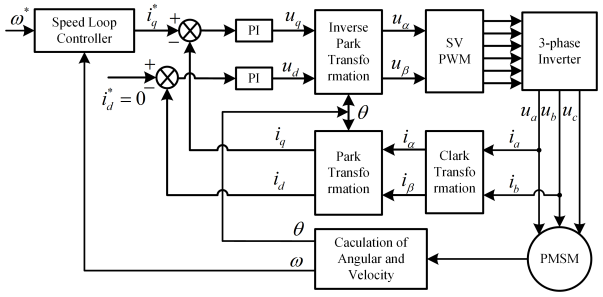

FIGURE 1. The FOC diagram of PMSM system by $i_d = 0$ control approach.

The remainder of this paper is organized as follows: Section II describes the mathematical model of PMSM vector control system. Section III introduces the details of the SMRL. In Section IV, the proposed SMC combining a disturbance torque observer, which is used to produce a feed-forward signal, is designed. Simulation and experimental studies of PMSM system are presented in Section V to verify the effectiveness of proposed approach. Finally, in Section VI, conclusions and a few future study directions are drawn.

II. MODEL OF THE CONTROL SYSTEM OF PMSM

It is assumed that the employed surface mounted PMSM has negligible cross coupling magnetic circuit saturation, hysteresis eddy current losses structural asymmetry, iron losses, and the sinusoidal magnetic field is distributed in space. In the rotor d-q coordinates, the dynamic mathematical model of a surface mounted PMSM (SPMSM), can be expressed as follows:

$$\begin{cases} u_d = R_s i_d + L_s i'_d - p_n \omega L_s i_q \\ u_q = R_s i_q + L_s i'_q - p_n \omega L_s i_d + p_n \omega \psi_f \\ J\omega' = 1.5 p_n \psi_f i_q - T_L - B\omega \end{cases} \tag{1}$$

where, u_d is the stator d-axis voltage, u_q is the stator q-axis voltage, i_d is the stator d-axis current, i_q is the stator q-axis current, i'_d, i'_q are first-order derivative of the stator d- and q-axis currents, L_s is the stator inductances, R_s is the stator resistance, ω is the rotor angular velocity,ω' is first-order derivative of the rotor angular velocity, p_n is the number of pole pairs, T_L is the load torque, ψ_f is the flux linkage, B is the viscous friction coefficient, and J is the moment of inertia.

Fig.1 shows the general field oriented control structure diagram of PMSM system by $i_d = 0$ control approach. There has one speed tracking loop controller and two current tracking loops controllers. In order to make the d-q axis currents stability, two conventional proportional-integral (PI) controllers are used in the two current loops. Generally, the i_d^* (d-axis reference current) is set to 0, and the i_q^* (q-axis reference current) is supplied by a speed controller. Speed and current of PMSM can be decoupled by the field oriented control

approach. This paper's objective is to design an improved SMC speed controller for the speed loop.

III. THE PROPOSED SLIDING MODE REACHING LAW

A. SLIDING SURFACE DESIGNED

SMC is a special nonlinear control approach with notable robustness in internal parameter variations and external disturbances rejection, compared with other control approaches. The design of SMC controller can be divided into two steps. Firstly, choose the sliding mode surface. Secondly, design the reaching law to force the system trajectory toward the sliding mode surface that ensures the system trajectory stay on the sliding mode surface.

The PMSM speed control system is a tracking system. The goal of the speed controller is to track the reference speed. Define the speed error as follows:

$$e = \omega^* - \omega \tag{2}$$

where,ω is actual rotor angular velocity of PMSM (obtained by the encoder) in time t, ω^* is the reference rotor angular velocity.

Choosing a linear sliding mode surface (sliding mode function) is:

$$s = cx_1 + x_2 \tag{3}$$

where, c is positive constant, x_1 is the speed error of PMSM, x_2 is first-order derivative of x_1.

$$\begin{cases} x_1 = e = \omega^* - \omega \\ x_2 = x_1' = -\omega' \end{cases} \tag{4}$$

When the states of system reached the sliding surface ($s = 0$), the system dynamics is represented as the following differential equation:

$$s = cx_1 + x_2 = ce + e' = 0 \tag{5}$$

The next work is to design an improved sliding mode reaching law, which forced the system trajectory to approach the sliding mode surface.

B. PROPOSED SMRL

Motivated by [16], the proposed SMRL is implemented based on the choice of piecewise function term.

The reaching law is set by:

$$s' = -f(x_1, x_2, s)\,\mathrm{sgn}(s) \tag{6}$$

$$f(x_1, x_2, s) = \begin{cases} \dfrac{k}{\varepsilon} & |x_1| > \delta \\ \dfrac{k\,|x_2|}{|x_1| + |x_2|} & |x_1| < \delta \end{cases} \tag{7}$$

where, $k > 0$, $\delta > 0$, and $0 < \varepsilon < 1$. x_1' is the state variable of system. $x_2 = x_1'$ is the derivative of the state variable. In this improved reaching law, it can be seen that if the system state is so far from the sliding mode surface, that the value of k/ε is more than the value of k. It has a faster reaching speed. When the system trajectory is close to the sliding mode surface, the$f(x_1, x_2, s) = k\,|x_2| \big/ (|x_1| + |x_2|)$, in which system state $|x_2|$ gradually approximates to zero, and the $f(x_1, x_2, s)$ gradually approximates to zero to restrains chattering. Therefore, the proposed SMC controller which is designed by this improved reaching law can not only suppress the chattering, but also has a faster reaching speed. This improved reaching law needs to be discretized, which will be applied by the digital signal processor. When the sliding mode surface is near to 0, the $f(x_1, x_2, s) = k\,|x_2| \big/ (|x_1| + |x_2|)$. According to the equation (6), discrete form of this improved reaching law is introduced as follows:

$$s(n+1) - s(n) = -\frac{k\,|x_2|\,T}{|x_1| + |x_2|}\mathrm{sgn}(s(n)) \tag{8}$$

In a finite time, assuming that the system trajectory arrives to the sliding mode surface from the $s > 0$, which shows that$s(n) = 0^+$. In the next period, the following equation can be obtained:

$$s(n+1) = -\frac{k\,|x_2|\,T}{|x_1| + |x_2|} \tag{9}$$

In a finite time, assuming that the system trajectory arrives to the sliding mode surface from the s <0, which shows that $s(n) = 0^-$. In the next period, the following equation can be obtained:

$$s(n+1) = \frac{k\,|x_2|\,T}{|x_1| + |x_2|} \tag{10}$$

Thus, the width of the discrete sliding mode band is:

$$\Delta = \frac{k\,|x_2|\,T}{|x_1| + |x_2|} \tag{11}$$

The bandwidth of discrete sliding mode is a formula for $|x_1|$, $|x_2|$. It can decrease as the decreasing system state $|x_1|$, which shows that state variables of system can reach the equilibrium point (0,0).

Consequently, the proposed reaching law can weaken the chattering phenomena effectively.

The discrete form of the conventional constant rate reaching law can be obtained:

$$s_1(n+1) - s_1(n) = -k_1 sgn(s_1(n)) \tag{12}$$

As a result, the bandwidth of discrete sliding mode for conventional constant rate reaching law is:

$$\Delta = k_1 T \tag{13}$$

Obviously, the bandwidth of conventional discrete sliding mode band is a constant. That means the system states will not reach the equilibrium state, which would produce the chattering between $k_1 T$ and $-k_1 T$.

The proposed reaching law has a substantial advantage over the conventional reaching law. The state trajectories of the conventional constant rate reaching law and the proposed reaching law are shown in Fig. 2.

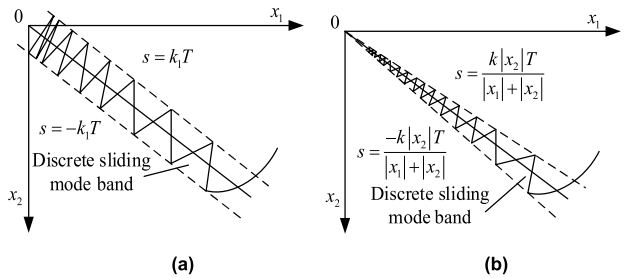

FIGURE 2. State trajectories of the conventional constant rate reaching law and the improved reaching law. (a) Constant rate reaching law. (b) Improved reaching law.

C. STABILITY ANALYSIS OF PROPOSED SMRL

To prove the stability of proposed reaching law, employing a Lyapunov function as:

$$V = \frac{s^2}{2} \tag{14}$$

The derivative of V is derived as:

$$\begin{aligned} V' &= ss' \\ &= = -sf\ (x_1, x_2, s)\ \mathrm{sgn}\ (s) \\ &= -|s| f\ (x_1, x_2, s) \\ &= \begin{cases} -\dfrac{k\,|s|}{\varepsilon} & |x_1| > \delta \\ -\dfrac{k\,|x_2|\,|s|}{|x_1| + |x_2|} & |x_1| < \delta \end{cases} \end{aligned} \tag{15}$$

where, $k > 0$, $\delta > 0$, and $0 < \varepsilon < 1$.

$$V' \leq 0 \tag{16}$$

In accordance with the Lyapunov stability theorem, V' is less than or equal to zero, which guarantee the system stable.

IV. DESIGN OF SMC SPEED CONTROLLER BASED ON PROPOSED REACHING LAW AND DTO

A. SPEED CONTROLLER OF PMSM BASED ON PROPOSED REACHING LAW

The lumped external disturbances and internal parameter variations always exist in the PMSM system. They will deteriorate the control effect of PMSM system. Therefore, a corresponding feed-forward compensation control approach should be added to suppress the disturbances.

From equations (1), the ideal motion equation of PMSM is:

$$\omega' = \frac{1.5 p_n \psi_f i_q}{J} - \frac{T_L}{J} - \frac{B\omega}{J} \tag{17}$$

In practical industrial applications, the PMSM is always affected by uncertainties of parameter variations and external disturbances. Considering the uncertainties of mathematical model of PMSM, equation (17) can be rewritten as:

$$\omega' = \left(\frac{1.5 p_n \psi_f i_q}{J} + \Delta 1\right) - \left(\frac{T_L}{J} + \Delta 2\right) - \left(\frac{B\omega}{J} + \Delta 3\right) + d \tag{18}$$

where, $\Delta 1$, $\Delta 3$ are the parameter variations, $\Delta 2$ is the load torque disturbance, d is the uncertain disturbance. Assuming, $g = d + \Delta 1 - \Delta 2 - \Delta 3 - T_L/J - B\omega/J$, which is the total disturbance. The largest disturbance is external load disturbance, and other disturbances can be ignored. Therefore, the total disturbance also can be expressed as: $g = -T_L/J$. The equation (19) with total disturbance can be expressed as:

$$\omega' = \frac{1.5 p_n \psi_f i_q}{J} + g \tag{19}$$

From the derivative of equation (5) and equation (6), equation (20) can be written as:

$$\begin{aligned} s' &= cx_2 + x_2' = -f\ (x_1, x_2, s)\ sgn\ (s) \\ s' &= -c\omega' - \omega'' = -f\ (x_1, x_2, s)\ sgn\ (s) \\ s' &= -c\left(\frac{1.5 p_n \psi_f i_q}{J} + g\right) - \frac{1.5 p_n \psi_f i_q'}{J} \\ &= -f\ (x_1, x_2, s)\ sgn\ (s) \end{aligned} \tag{20}$$

Thus, the control input i_q^* is designed as follows:

$$\begin{aligned} i_q^* &= \frac{1}{D}\int \left[-c\omega' - k_g \hat{g} + f\ (x_1, x_2, s)\ sgn\ (s)\right] d\tau \\ &= \frac{1}{D}\int \left[-c\omega' + k_t \hat{T}_L + f\ (x_1, x_2, s)\ sgn\ (s)\right] d\tau \end{aligned} \tag{21}$$

where, $D = 1.5 p_n \psi_f$, $k_t = k_g/J$ is the gain of feed-forward, the estimation value of g is $\hat{g} = -\hat{T}_L/J$. $\hat{T}_L$ is the estimate value of disturbance torque.

B. DISTURBANCE TORQUE OBSERVER

From the previous section, the disturbance torque observer is used to estimate the $\hat{T}_L$. When the sampling frequency of the controller is very high, it can be approximate that the load torque T_L is a constant during a sampling period. According to the motion equations of PMSM, it can be expressed as follows:

$$\begin{cases} T_e = J\omega' + B\omega + T_L \\ \theta' = \omega \\ T_L' = 0 \end{cases} \tag{22}$$

which can also be expressed as follows:

$$\begin{cases} x' = Ax + Du \\ y = Cx \end{cases} \tag{23}$$

where x, A, D, u and y are given by:

$$x = \begin{bmatrix} \theta \\ \omega \\ T_L \end{bmatrix}, \quad A = \begin{bmatrix} 0 & 1 & 0 \\ 0 & -\frac{B}{J} & -\frac{1}{J} \\ 0 & 0 & 0 \end{bmatrix}, \quad D = \begin{bmatrix} 0 \\ \frac{1}{J} \\ 0 \end{bmatrix},$$
$$u = T_e, \quad C = [1 \quad 0 \quad 0], \quad y = \theta.$$

The disturbance torque observer is designed by the idea of reduced-order:

$$\begin{bmatrix} \hat{\omega}' \\ \hat{T}_L' \end{bmatrix} = \begin{bmatrix} -\frac{B}{J} & -\frac{1}{J} \\ 0 & 0 \end{bmatrix} \begin{bmatrix} \hat{\omega} \\ \hat{T}_L \end{bmatrix} + \begin{bmatrix} -\frac{1}{J} \\ 0 \end{bmatrix} T_e + \begin{bmatrix} k_1 \\ k_2 \end{bmatrix} (\omega - \hat{\omega}) \tag{24}$$

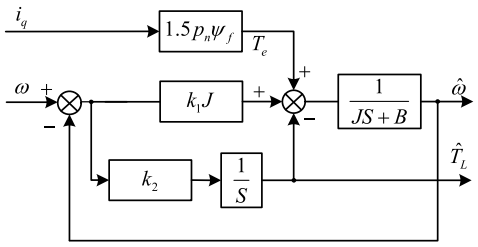

FIGURE 3. The block diagram of disturbance torque observer.

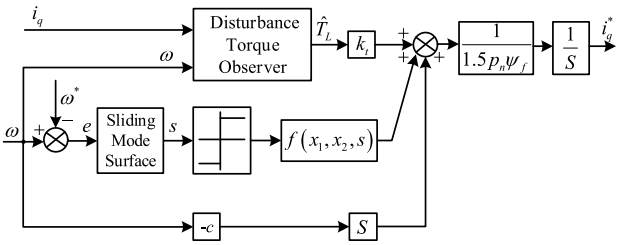

FIGURE 4. The control structure of SMC+DTO.

TABLE 1. Parameter setting of the PMSM.

Parameter	Symbol	Value
Rated Voltage	V	36 V
Rated Current	I	4.6 A
Maximum Current	I_{max}	13.8 A
Rated Power	P	100 W
Rated Torque	T	0.318 N.m
Stator Phase Resistance	R	0.375 Ohm
Motor Inertia	J	0.0588 kg.m^2.10^{-4}
Pole Pairs	P_n	4 Pair
q-axis Inductance	L_q	0.001 H
d-axis Inductance	L_d	0.001 H
Incremental Encoder Lines	N	2500PPR

where, k_1,k_2 are the state feedback coefficients. $\hat{T}_L$ is the estimate value of disturbance torque. $\hat{\omega}$ is the estimate value of rotor angular velocity.

The disturbance torque observer can be written as:

$$\begin{cases} \hat{x'}_0 = A_0\hat{x} + D_0u_0 + K_e\left[y_0 - \hat{y}_0\right] \\ \hat{y}_0 = C_0\hat{x}_0 \end{cases} \tag{25}$$

where $\hat{x}_0$, A_0, D_0, u_0,K_e,C_0,$\hat{y}_0$ and y_0 are given by:

$$\hat{x}_0 = \begin{bmatrix} \hat{\omega} \\ \hat{T}_L \end{bmatrix},\ A_0 = \begin{bmatrix} -\frac{B}{J} & -\frac{1}{J} \\ 0 & 0 \end{bmatrix},\ D_0 = \begin{bmatrix} \frac{1}{J} \\ 0 \end{bmatrix},$$
$$K_e = \begin{bmatrix} k_1 \\ k_2 \end{bmatrix}, u_0 = T_e,\ C_0 = [1 \quad 0],\ \hat{y}_0 = \hat{\omega},\ y_0 = \omega. \tag{26}$$

The characteristic equation of the observer is [28]:

$$\det\left[sI - (A_0 - K_eC_0)\right] = 0 \tag{27}$$

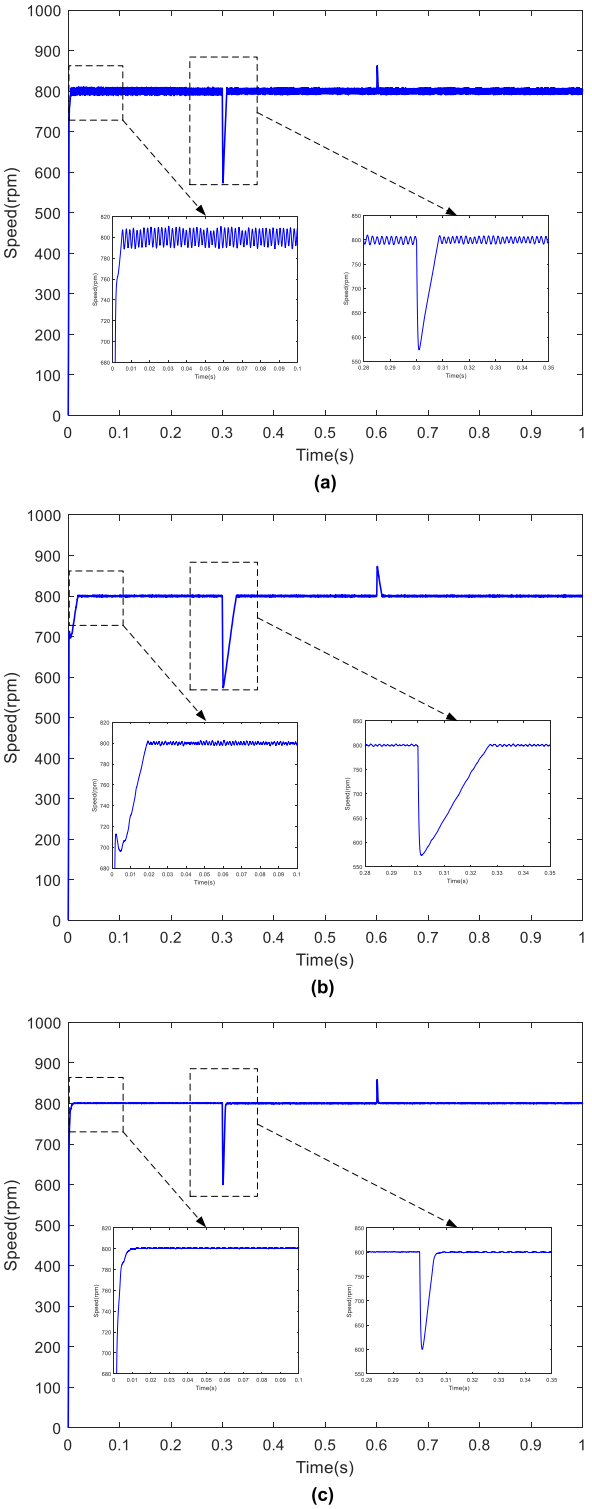

FIGURE 5. Simulation responses of speed in the presence of load torque disturbance at 800 rpm. (a) SMC based on constant rate reaching law with k = 8000000. (b) SMC based on constant rate reaching law with k = 2000000. (c) SMC based on proposed reaching law with k = 2000000.

To ensure the disturbance torque observer is stable, the selection of the gain matrix K_e is important. The block diagram of disturbance torque observer is shown in Fig.3.

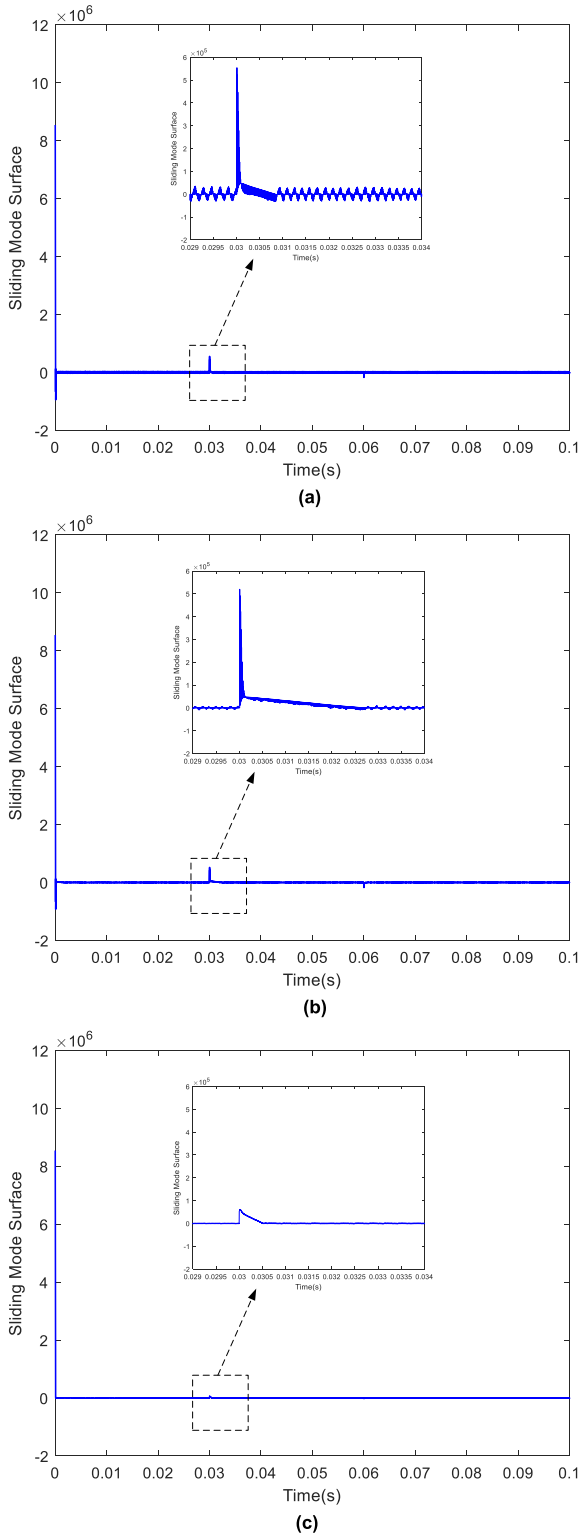

FIGURE 6. Simulation responses of sliding mode surface in the presence of load torque disturbance at 800 rpm. (a) SMC based on constant rate reaching law with k = 8000000. (b) SMC based on constant rate reaching law with k = 2000000. (c) SMC based on proposed reaching law with k = 2000000.

The composite control method combining an improved SMRL and a feed-forward signal produced by disturbance torque observer applied to the speed control loop is shown in Fig.4.

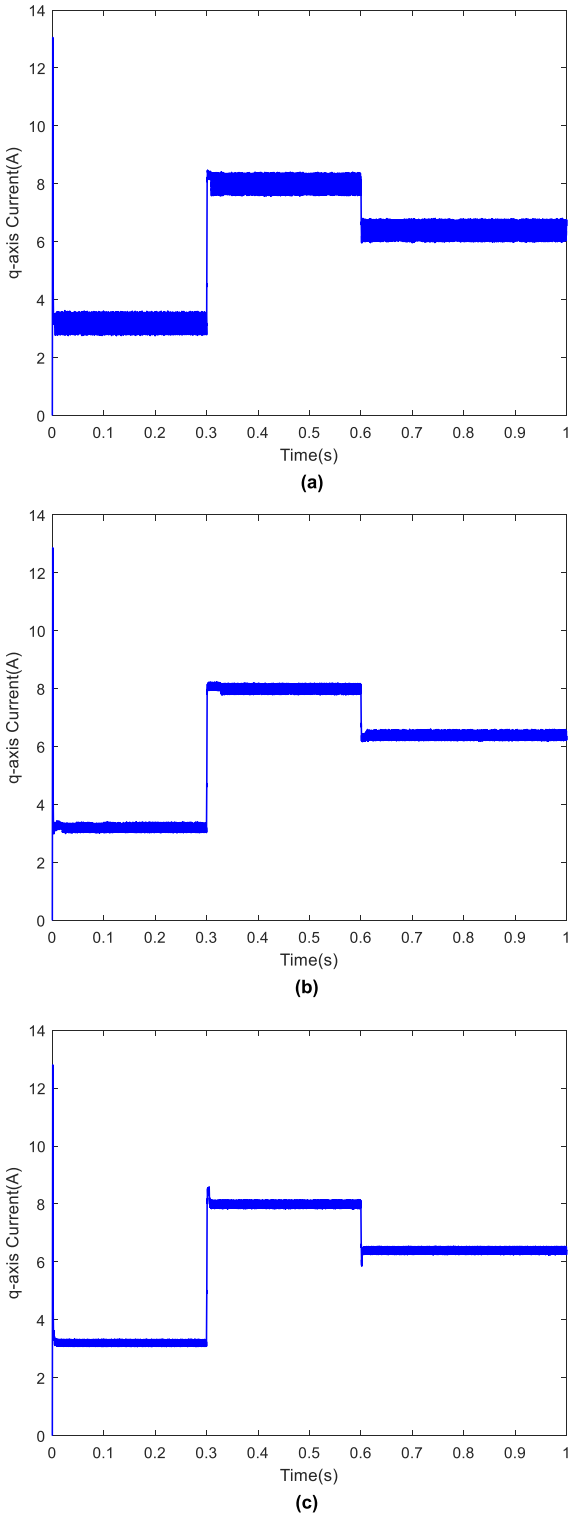

FIGURE 7. Simulation responses of q-axis current in the presence of load torque disturbance at 800 rpm. (a) SMC based on constant rate reaching law with k = 8000000. (b) SMC based on constant rate reaching law with k = 2000000. (c) SMC based on proposed reaching law with k = 2000000.

V. SIMULATION AND EXPERIMENTAL RESULTS

For the purpose of illustrating the feasibility of the proposed strategy, the simulation and experimental studies on the speed control system of PMSM are carried out.

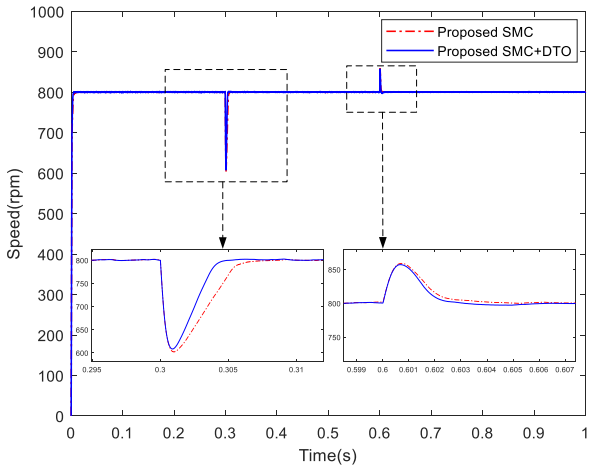

FIGURE 8. Simulation responses of speed under proposed SMC and proposed SMC+DTO approaches in the presence of load torque disturbance at 800 rpm.

A. NUMERICAL SIMULATION

A field oriented control system model of PMSM based on proposed speed controller is built in Simulink2018a. PMSM parameters for the simulation are listed in table 1.

In q-axis current PI controller, the proportional gain is $L_q \cdot lambda$ and the integral gain is $R \cdot lambda$, $lambda = 9000$. The q-axis reference current i_q^* is limited in ± 10 A. In d-axis current PI controller, the proportional gain is $L_d \cdot lambda$ and the integral gain is $R \cdot lambda$. The nominal values of SMC controller based on proposed reaching law: $k = 2000000$; $\varepsilon = 0.2$; $\delta = 3$; $c = 2000$.

The simulation results of the SMC approach based on constant rate reaching law with $k = 8000000$, the SMC approach based on constant rate reaching law with $k = 2000000$, and the proposed SMC approach based on improved reaching law with $k = 2000000$ are shown in Figs. 5, 6 and 7, respectively. The initial load of PMSM is 0.2N.m. A load torque 0.5N.m is applied at 0.3s, then, the load torque decrease to 0.4N.m at 0.6s.

Figs. 5(a), 5(b), and 5(c) show the dynamic responses of PMSM speed. It can also be seen that the reference speed is 800 rpm, the SMC approach based on constant rate reaching law with $k = 8000000$ has a quicker response time than the SMC approach based on constant rate reaching law with $k = 2000000$. However, it has a bigger chattering than the SMC approach based on constant rate reaching law with $k = 2000000$. Small sliding mode gain can reduce chattering phenomenon, but with long reaching time. Reaching time to sliding mode surface and chattering is the main contradiction of constant rate reaching law. The SMC approach based on proposed reaching law cannot only reduce the chattering but also has a fast reaching time. Figs. 6(a), 6(b), and 6(c) show dynamic responses of sliding mode surface. Figs. 7(a), 7(b), and 7(c) show dynamic responses of PMSM q-axis current. It can be seen from the simulation results, the proposed SMC approach based on proposed reaching law can ensure smaller chattering and faster reaching time than the conventional SMC approach does.

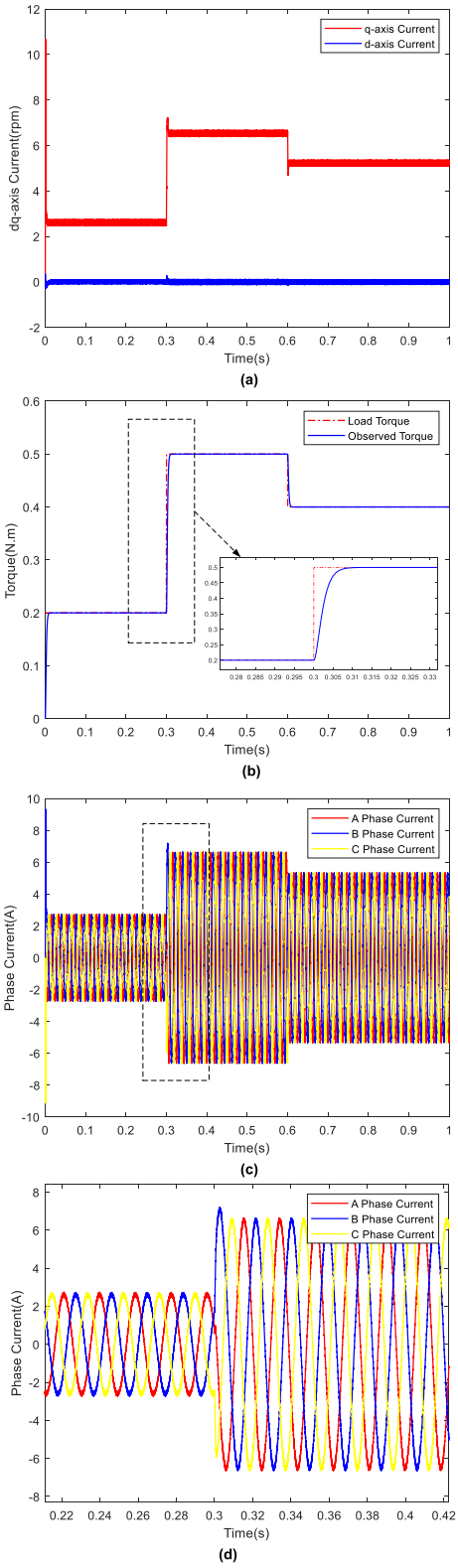

FIGURE 9. Simulation results of proposed SMC+DTO in the case of load torque disturbance at 800 rpm. (a)i_d and i_q currents. (b) Observed disturbance torque. (c) Phase currents. (d) Partial enlarged detail of phase currents.

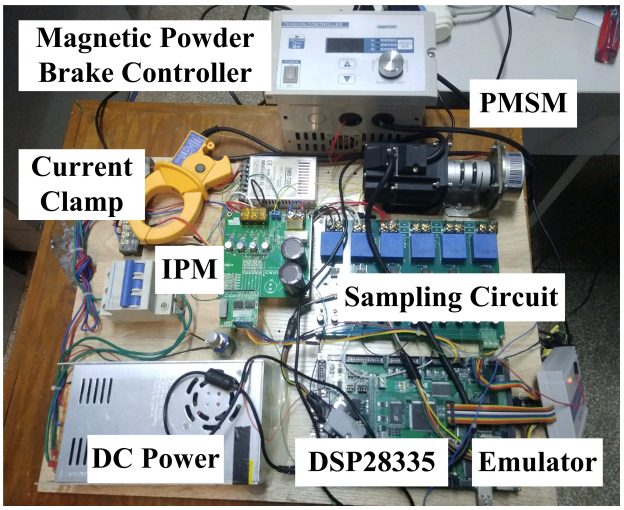

FIGURE 10. Photograph of the experimental setup.

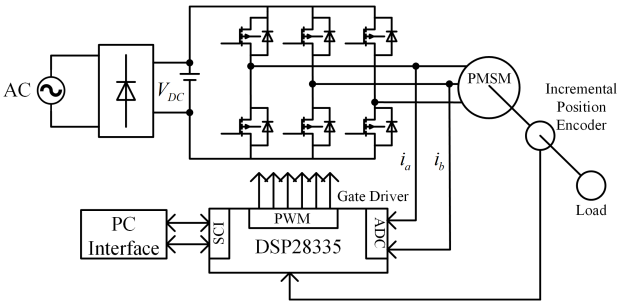

FIGURE 11. Configuration of the experimental system.

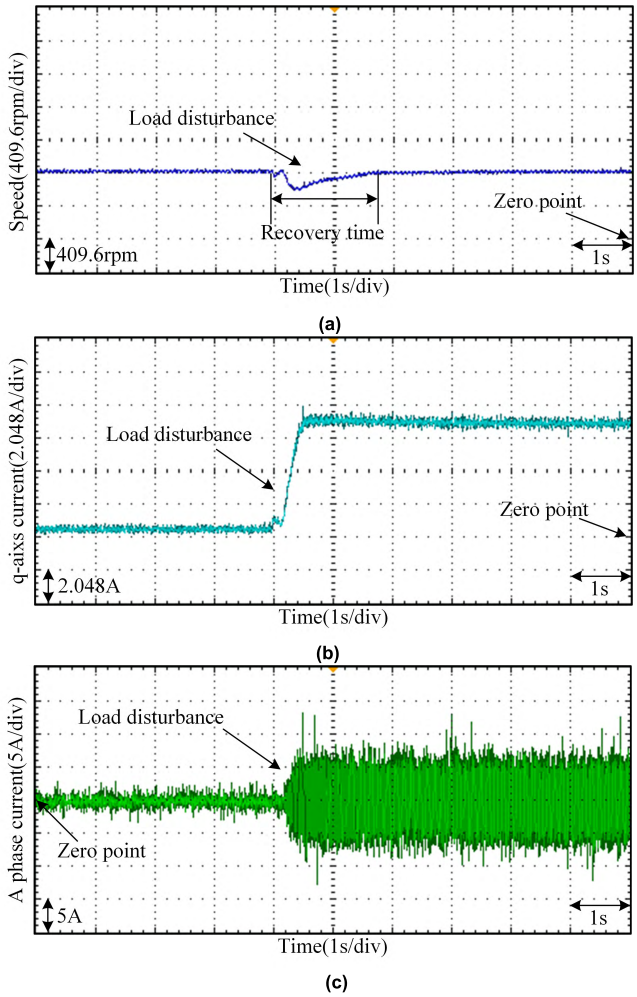

FIGURE 12. Experimental results of proposed SMC in the case of load torque disturbance at 800 rpm. (a) Speed. (b)i_q.(c) A phase current.

The composite control method combining an improved SMRL and a feed-forward signal produced by disturbance torque observer is simulated in Matlab2018a. The nominal values of SMC+DTO approach based on proposed reaching law: $k = 2000000$; $\varepsilon = 0.2$; $\delta = 3$; $c = 2000$; $k_t = 5$;$k_1 = 1200$;$k_2 = -2.1168$. The nominal values of SMC approach based on proposed reaching law without a feed-forward signal compensation are same as SMC+DTO approach: $k = 2000000$; $\varepsilon = 0.2$; $\delta = 3$; $c = 2000$.

Fig.8 shows that the speed response under SMC approach based on proposed reaching law and SMC+DTO approach based on proposed reaching law in the presence of load torque disturbance at 800 rpm. It can be seen that the speed-loop of PMSM has a better robust performance after a feedforward compensation signal produced by DTO.

Fig.9(a) shows the dynamic response of d-q-axis currents of the proposed SMC+DTO. The load torque added suddenly at 0.3s, then the load torque decreased at 0.6s. The d-q axis currents can vary quickly according to the load torque characteristics. Fig.9(b) shows the magnitude of observed disturbance torque. Fig.9(c) shows the dynamic response of phase currents. Fig.9(d) shows the partial enlarged detail of phase currents.

B. EXPERIMENTAL RESULTS

The photograph of the experimental setup including PMSM, driver module, sampling module, DSP28335 core board, magnetic powder brake controller and the emulator is shown in Fig.10.

A floating-point DSP TMS320F28335, which is designed by TI Company, is the kernel of DSP28335 core board. Moreover, analog to digital converter (ADC) AD7606, pulse width modulation (PWM), digital to analog converter (DAC) AD5344, and encoder interface circuit are contained in the DSP 28335 core board. Intelligent power module (PS21965) produced by Mitsubishi Corporation, is used to drive the PMSM. Hall sensors, which are produced by LEM Company, are used to measure phase currents of PMSM. The PMSM integrates the incremental position encoder of 2500 lines, which is used to get the rotor speed and position measured signals. Furthermore, the proposed control strategies that include SVPWM are programmed in the DSP by the 'C' code using the main program and one PWM interrupt service program. All the programs are developed in the Code Composer

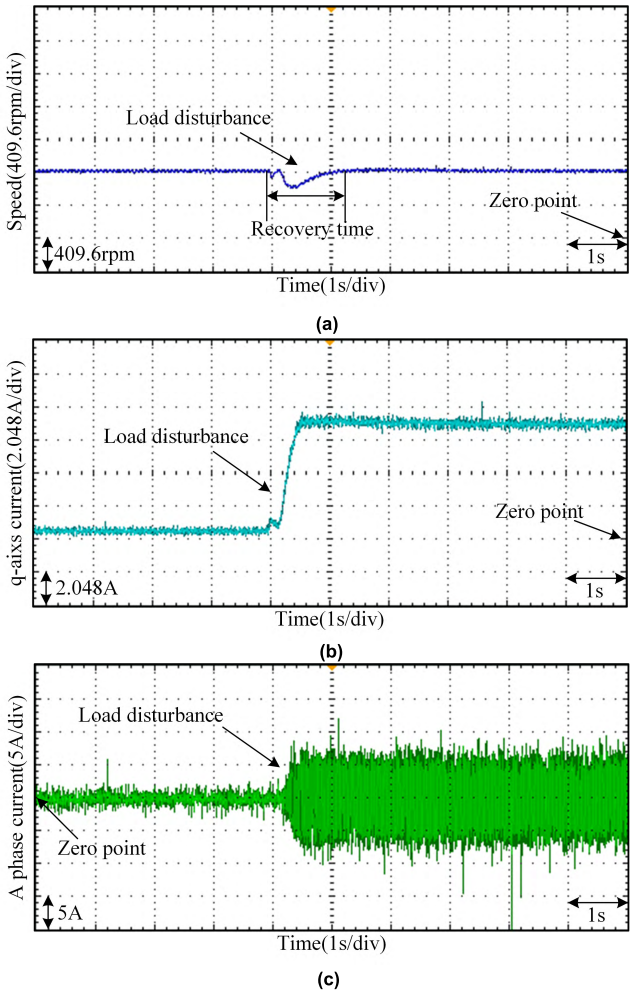

FIGURE 13. Experimental results of proposed SMC+DTO in the case of load torque disturbance at 800 rpm. (a) Speed. (b)i_q. (c) A phase current.

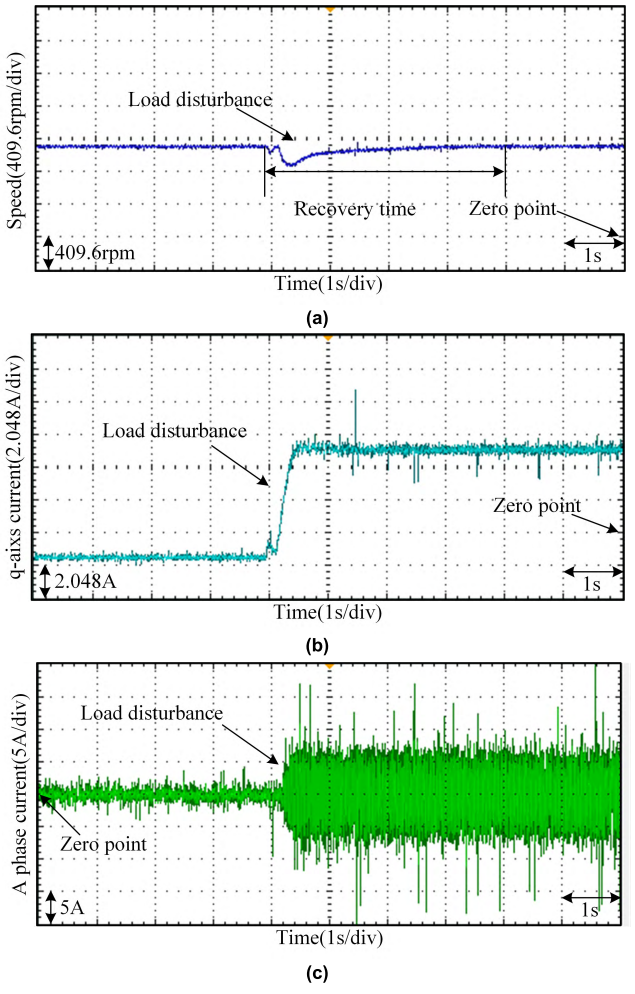

FIGURE 14. Experimental results of SMC based on conventional constant rate reaching law in the case of load torque disturbance at 1100 rpm. (a) Speed. (b)i_q. (c) A phase current.

Studio IDE (CCS6.2) and then downloaded to the RAM of the DSP. The experimental results are output to the oscilloscope through DAC. Fig.11 depicts the configuration of the experimental system. The parameters of PMSM are equal to that in Table 1. The experimental parameters of SMC+DTO controller are as follows:$k = 2000000$; $\varepsilon = 0.2$; $\delta = 3$; $c = 2000$; $k_t = 3$;$k_1 = 1200$; $k_2 = -2.1168$. Where the value of k_t is a little different from the simulation.

Parameters of both PI controllers of current loops are equal: the proportional gain is 0.2, and the integral gain is 0.006. The speed loop sampling frequency is 5000 Hz , the current loop sampling frequency is same as the speed loop. The clock frequency of DSP28335 is 150 MHz. Two kinds of reference speed, which are 800 rpm and 1100 rpm, are used to verify the performance of the proposed SMC+DTO control strategy.

Fig. 12 depicts the experimental results of the proposed SMC controller based on the proposed reaching law in the case of load torque disturbance at 800 rpm. Fig. 12(a) depicts the dynamic responses of PMSM speed by the proposed SMC strategy at 800 rpm. Fig. 12(b) depicts the dynamic responses of q-axis current by the proposed SMC strategy at 800 rpm. Fig. 12(c) depicts the dynamic responses of PMSM's A phase current by the proposed SMC strategy at 800 rpm.

Fig. 13 shows the experimental results of the proposed SMC+DTO controller with a feed-forward signal produced by DTO in the case of load torque disturbance at 800 rpm. Fig. 13(a) depicts the dynamic responses of PMSM speed by the proposed SMC+DTO strategy at 800 rpm. Fig. 13(b) depicts the dynamic responses of q-axis current by the proposed SMC+DTO strategy at 800 rpm. Fig. 13(c) depicts the dynamic responses of PMSM's A phase current by the proposed SMC+DTO strategy at 800 rpm. It can be seen from the experimental results that the proposed SMC+DTO strategy, has higher disturbance rejection potential, with much shorter recovery time towards load disturbance.

Fig. 14 depicts the experimental results of the SMC controller based on conventional constant rate reaching law in the case of load torque disturbance at 1100 rpm. The experimental parameters of SMC based on conventional constant rate

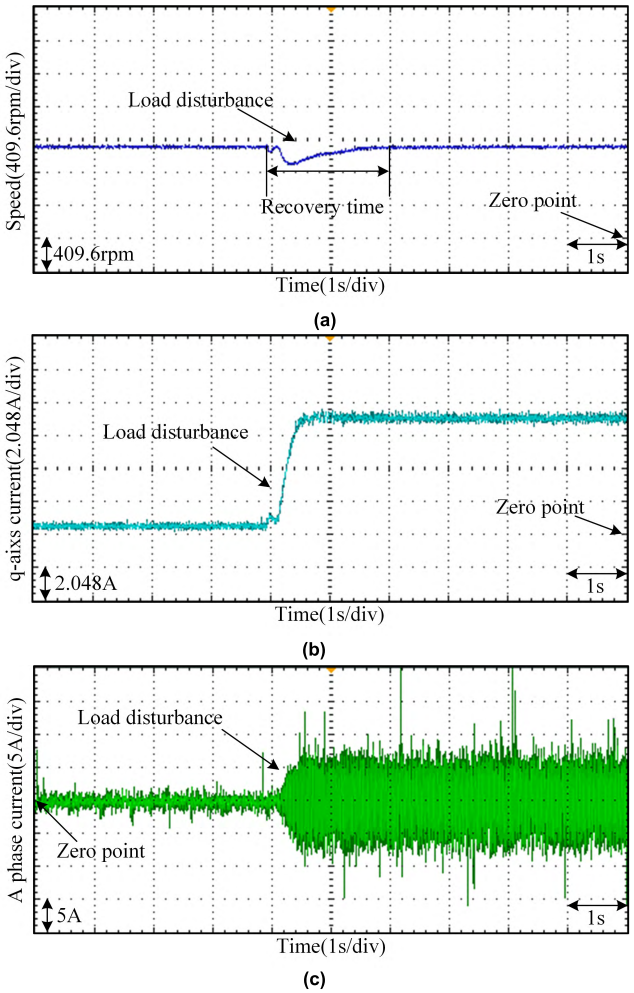

FIGURE 15. Experimental results of proposed SMC in the case of load torque disturbance at 1100 rpm. (a) Speed. (b)i_q. (c) A phase current.

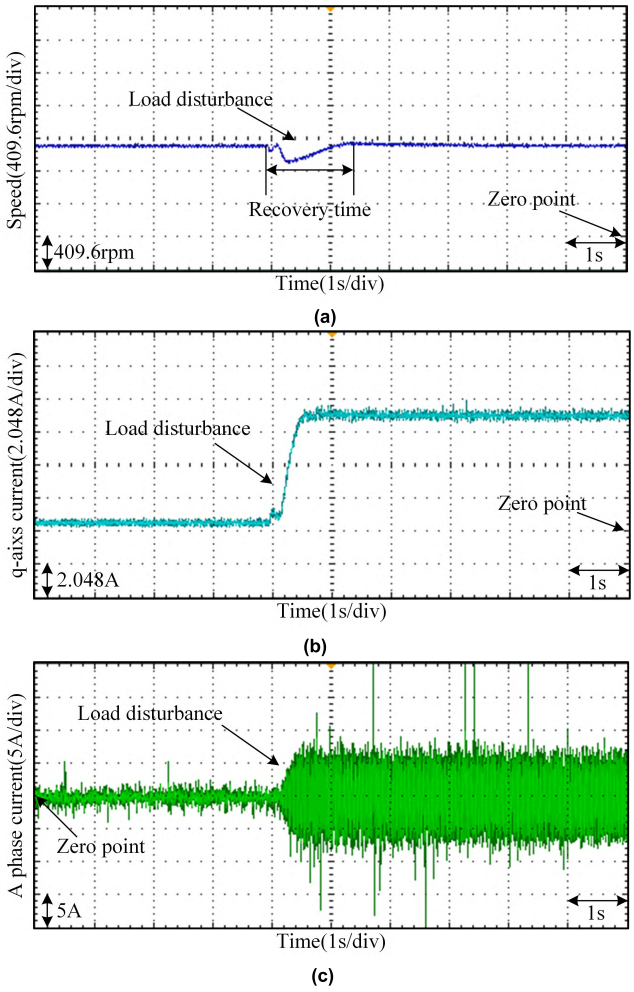

FIGURE 16. Experimental results of proposed SMC+DTO in the case of load torque disturbance at 1100 rpm. (a) Speed. (b)i_q. (c) A phase current.

reaching law are same as SMC based on proposed reaching law with $k = 2000000$. Fig. 14(a) depicts the dynamic responses of PMSM speed by SMC strategy based on conventional constant rate reaching law at 1100 rpm. Fig. 14(b) depicts the dynamic responses of q-axis current by SMC strategy based on conventional constant rate reaching law at 1100 rpm. Fig. 14(c) depicts the dynamic responses of PMSM's A phase current by SMC strategy based on conventional constant rate reaching law at 1100 rpm.

Fig. 15 depicts the experimental results of the proposed SMC controller based on the proposed reaching law in the case of load torque disturbance at 1100 rpm. Fig. 15(a) depicts the dynamic responses of PMSM speed by the proposed SMC strategy at 1100 rpm. Fig. 15(b) depicts the dynamic responses of q-axis current by the proposed SMC strategy at 1100 rpm. Fig. 15(c) depicts the dynamic responses of PMSM's A phase current by the proposed SMC strategy at 1100 rpm.

From Fig.14 and Fig.15, it is clear that the reference speed is 1100 rpm, the SMC approach based on constant rate reaching law with $k = 2000000$ has a longer response time than the SMC approach based on proposed reaching law with $k = 2000000$.

Fig. 16 depicts the experimental results of the proposed SMC+DTO controller based on proposed reaching law with a feed-forward signal produced by DTO in the case of load torque disturbance at 1100 rpm. Fig. 16(a) depicts the dynamic responses of PMSM speed by the proposed SMC+DTO strategy at 1100 rpm. Fig. 16(b) depicts the dynamic responses of q-axis current by the proposed SMC+DTO strategy at 1100 rpm. Fig. 16(c) depicts the dynamic responses of PMSM's A phase current by the proposed SMC+DTO strategy at 1100 rpm. It can be found that compared with the experimental results at 800 rpm, the proposed SMC+DTO controller has a longer recovery time at 1100 rpm. However, the proposed SMC+DTO strategy can also have a better performance and more precise disturbance rejection capacity than the SMC controller without a feed-forward signal produced by DTO. Fig.17 shows the magnitude of experimental observed disturbance torque.

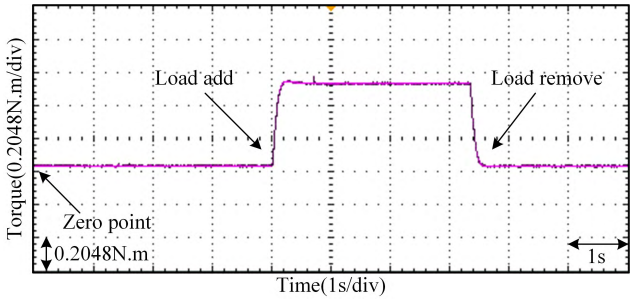

FIGURE 17. Observed disturbance torque of PMSM (experiment).

VI. CONCLUSION

In this study, for the purpose of optimizing the speed control performance of the PMSM closed-loop system, detailed design and implementation course of SMC+DTO speed controller are presented. At the beginning, the dynamics model of the PMSM and the field oriented control approach were described. Moreover, improved reaching law is selected. Then, a composite PMSM speed control method combining the proposed SMRL and DTO, called SMC+DTO is derived in detail. Furthermore, the proposed control strategy was implemented in Matlab2018a and TMS320F28335. Finally, effectiveness of the proposed controller is verified by the simulation and experimental results.

Perspectives for future research are listed as follows: 1) Only external load disturbance can be observed, but internal parameters disturbance cannot be observed by DTO. Therefore, a new observer needs to be explored in future work. 2) The proposed SMC+DTO controller should be proved mathematically as a whole. 3) Further investigation can be underway to expand the proposed SMRL to sliding mode observer for sensorless control of PMSM.

REFERENCES

[1] P. C. Krause, O. Wasynczuk, and S. D. Sudhoff, *Analysis of Electric Machinery and Drive Systems*. New York, NY, USA: Wiley, 1995.

[2] J.-W. Jung, V. Q. Leu, T. D. Do, E.-K. Kim, and H. H. Choi, "Adaptive PID speed control design for permanent magnet synchronous motor drives," *IEEE Trans. Power Electron.*, vol. 30, no. 2, pp. 900–908, Feb. 2015.

[3] A. Al-Janabi, *Vector Control of Permanent Magnet Synchronous Motor: LEARN Types of Motors and Application. The PMSM Motor Applications. MATLAB Simulation of PMSM With Vector Control Idea*. Saarbrücken, Germany: LAP LAMBERT Academic, 2016.

[4] C.-K. Lai and K.-K. Shyu, "A novel motor drive design for incremental motion system via sliding-mode control method," *IEEE Trans. Ind. Electron.*, vol. 52, no. 2, pp. 499–507, Apr. 2005.

[5] H. Chaoui and P. Sicard, "Adaptive fuzzy logic control of permanent magnet synchronous machines with nonlinear friction," *IEEE Trans. Ind. Electron.*, vol. 59, no. 2, pp. 1123–1133, Feb. 2012.

[6] H. Aschemann and D. Schindele, "Sliding-mode control of a high-speed linear axis driven by pneumatic muscle actuators," *IEEE Trans. Ind. Electron.*, vol. 55, no. 11, pp. 3855–3864, Nov. 2008.

[7] X. Zhang, B. Hou, and Y. Mei, "Deadbeat predictive current control of permanent-magnet synchronous motors with stator current and disturbance observer," *IEEE Trans. Power Electron.*, vol. 32, no. 5, pp. 3818–3834, May 2017.

[8] F. F. M. El-Sousy, "Intelligent optimal recurrent wavelet Elman neural network control system for permanent-magnet synchronous motor servo drive," *IEEE Trans. Ind. Informat.*, vol. 9, no. 4, pp. 1986–2003, Nov. 2013.

[9] F. F. M. El-Sousy, "Adaptive dynamic sliding-mode control system using recurrent RBFN for high-performance induction motor servo drive," *IEEE Trans Ind. Informat.*, vol. 9, no. 4, pp. 1922–1936, Nov. 2013.

[10] X. Song, J. Fang, B. Han, and S. Zheng, "Adaptive compensation method for high-speed surface PMSM sensorless drives of EMF-based position estimation error," *IEEE Trans. Power Electron.*, vol. 31, no. 2, pp. 1438–1449, Feb. 2016.

[11] V. Repecho, D. Biel, and A. Arias, "Fixed switching period discrete-time sliding mode current control of a PMSM," *IEEE Trans. Ind. Electron.*, vol. 65, no. 3, pp. 2039–2048, Mar. 2018.

[12] J. V. Gorp, M. Defoort, M. Djemai, and K. C. Veluvolu, "Fault detection based on higher-order sliding mode observer for a class of switched linear systems," *IET Control Theory Appl.*, vol. 9, no. 15, pp. 2249–2256, Oct. 2015.

[13] J. J. Rath, M. Defoort, H. R. Karimi, and K. C. Veluvolu, "Output feedback active suspension control with higher order terminal sliding mode," *IEEE Trans. Ind. Electron.*, vol. 64, no. 2, pp. 1392–1403, Feb. 2017.

[14] G. Sun, Z. Ma, and J. Yu, "Discrete-time fractional order terminal sliding mode tracking control for linear motor," *IEEE Trans. Ind. Electron.*, vol. 65, no. 4, pp. 3386–3394, Apr. 2018.

[15] H. Ma, J. Wu, and Z. Xiong, "Discrete-time sliding-mode control with improved quasi-sliding-mode domain," *IEEE Trans. Ind. Electron.*, vol. 63, no. 10, pp. 6292–6304, Oct. 2016.

[16] X. Zhang, L. Sun, K. Zhao, and L. Sun, "Nonlinear speed control for PMSM system using sliding-mode control and disturbance compensation techniques," *IEEE Trans. Power Electron.*, vol. 28, no. 3, pp. 1358–1365, Mar. 2013.

[17] X. Yu, B. Wang, and X. Li, "Computer-controlled variable structure systems: The state-of-the-art," *IEEE Trans. Ind. Informat.*, vol. 8, no. 2, pp. 197–205, May 2012.

[18] W. Gao and J. C. Hung, "Variable structure control of nonlinear systems: A new approach," *IEEE Trans. Ind. Electron.*, vol. 40, no. 1, pp. 45–55, Feb. 1993.

[19] W. Gao, Y. Wang, and A. Homaifa, "Discrete-time variable structure control systems," *IEEE Trans. Ind. Electron.*, vol. 42, no. 2, pp. 117–122, Apr. 1995.

[20] M. P. Aghababa, "Design of hierarchical terminal sliding mode control scheme for fractional-order systems," *IET Sci., Meas. Technol.*, vol. 9, no. 1, pp. 122–133, Jan. 2015.

[21] Q. Xu, "Digital sliding-mode control of piezoelectric micropositioning system based on input–output model," *IEEE Trans. Ind. Electron.*, vol. 61, no. 10, pp. 5517–5526, Oct. 2014.

[22] R. K. Munje, B. M. Patre, and A. P. Tiwari, "Discrete-time sliding mode spatial control of advanced heavy water reactor," *IEEE Trans. Control Syst. Technol.*, vol. 24, no. 1, pp. 357–364, Jan. 2016.

[23] S. Qu, X. Xia, and J. Zhang, "Dynamics of discrete-time sliding-mode-control uncertain systems with a disturbance compensator," *IEEE Trans. Ind. Electron.*, vol. 61, no. 7, pp. 3502–3510, Jul. 2014.

[24] A. Bartoszewicz and P. Leśniewski, "New switching and nonswitching type reaching laws for SMC of discrete time systems," *IEEE Trans. Control Syst. Technol.*, vol. 24, no. 2, pp. 670–677, Mar. 2016.

[25] H. Ma, J. Wu, and Z. Xiong, "A novel exponential reaching law of discrete-time sliding-mode control," *IEEE Trans. Ind. Electron.*, vol. 64, no. 5, pp. 3840–3850, May 2017.

[26] I. Yazici and E. K. Yaylaci, "Maximum power point tracking for the permanent magnet synchronous generator-based WECS by using the discrete-time integral sliding mode controller with a chattering-free reaching law," *IET Power Electron.*, vol. 10, no. 13, pp. 1751–1758, Oct. 2017.

[27] S. M. Mozayan, M. Saad, H. Vahedi, H. Fortin-Blanchette, and M. Soltani, "Sliding mode control of PMSG wind turbine based on enhanced exponential reaching law," *IEEE Trans. Ind. Electron.*, vol. 63, no. 10, pp. 6148–6159, Oct. 2016.

[28] S. K. Kommuri, S. B. Lee, and K. C. Veluvolu, "Robust sensors-fault-tolerance with sliding mode estimation and control for PMSM drives," *IEEE/ASME Trans. Mechatronics*, vol. 23, no. 1, pp. 17–28, Feb. 2018.

Authors' photographs and biographies not available at the time of publication.